

# Study of the linear behaviour of a PSC containment dome with large openings

K. Murali Mohan <sup>a</sup>, Sekhar K. Chakrabarti <sup>a,\*</sup>, Prabir C. Basu <sup>b</sup>,  
Siddhartha Ghosh <sup>a</sup>

<sup>a</sup> Department of Civil Engineering, Indian Institute of Technology, Kanpur 208026, India

<sup>b</sup> Civil and Structural Engineering Division, Atomic Energy Regulatory Board, Mumbai 400094, India

Received 17 September 1999; accepted 15 October 1999

## 1. Introduction

Assurance of safety of public and workers, and also protection of environment against unacceptable radiological hazards, are the principal objectives in the design, construction and operation of a nuclear containment structure. These criteria are to be met during both normal operating and accident conditions of the nuclear power plant. India's Nuclear Power Plant (NPP) program, based on Pressurized Heavy Water Reactor (PHWR), started in the late 1960s. Through the years, also with other safety systems, the design of PHWR containment systems in India has undergone progressive improvement to enhance its reliability and effectiveness. The containment design of Indian PHWR based NPP has been developed using a complete double containment philosophy. The principal design criteria for containment arise out of Design Basis Accidents (DBA) such as Loss of Coolant Accident (LOCA) and Main Steam Line Break (MSLB) and it has to achieve a specified level of leaktightness under these conditions.

The structural arrangement of a reactor building of a typical Indian PHWR consists of two containments; inner (primary) and outer (secondary) (Warudkar, 1997; Chakrabarti and Basu, 1999). Both the containment structures have vertical cylindrical wall and segmented spherical dome as cap; and they rest on a common reinforced concrete base raft. The inner containment (IC) structure is made of prestressed concrete (PSC) while the outer one is made of reinforced concrete (RC). Both the PSC IC dome and RC outer containment (OC) dome have got four major circular (in plan) openings in them, which are called steam generator (SG) openings and are sealed with dished heads after erection of the SGs. This is the unique feature of the containment structure of a PHWR based Indian NPP.

The finite element analytical study on distribution of stresses around the equipment hatch opening of a PSC containment wall, under internal pressure and prestress, by Harrop (1984), shows that it is a zone of stress concentration. The loads together produce compressive membrane local hoop stresses around the opening, and some tensile extreme fiber hoop stresses which attain the tensile stress limit of concrete under increased internal pressure. An overview of the state-of-the-

\* Corresponding author. Tel.: +91-512-597173; fax: +91-512-590260, 597395, 590007.

E-mail address: chakra@iitk.ac.in (S.K. Chakrabarti)

art of containment capability by the ASCE Committee (Task Group on Containment Capability, 1984) reported that the local strains at the periphery of a large opening vary from point to point causing an ovaling of the opening. It also describes the decrease in stiffness of the structure at stages; due to increasing cracks in concrete, then the yielding of the reinforcements, and lastly the yielding of the tendons; thus producing a multi-stage load-deformation curve for the structure under monotonic increment of pressure loading. It is observed that there has been no significant work to study the behaviour of PSC containment domes with large openings. Chakrabarti et al. (1994, 1997) addressed the issue of leakage through the steel concrete interface at the embedded parts of the SG openings in the IC dome of a typical Indian PHWR, considering the strength development mechanism in concrete at different depths from the embedded plate, and also the issue of permeability at and around the interface. In the work presented here, attempts have been made to know the linear behaviour of the PSC IC dome having large SG openings, under predominant design loading conditions, analytically. The

work, primarily, was intended for knowing the dome response at and around the openings.

## 2. Structural arrangement of the inner containment

As it was stated earlier the Indian PHWR program has been emphasizing on the double containment philosophy from its very beginning. This has led to most of the reactor containment structures of this country being designed as double wall containment systems. Warudkar (1997) discussed in detail the structural configuration of the containment of Indian NPP. This double wall concept ensures the desired safety levels for effective accident mitigation, by branching the main operation requirements in the following manner.

1. The IC is designed to withstand pressure and temperature conditions during accidents and seismic effects, with specific leakage provisions.
2. The OC is designed against aircraft/missile impact, seismic/wind loads and a small overpressure or underpressure due to accident conditions.
3. The annular space between the two walls is used to collect and filter residual radioactive leakage (especially for highly hypothetical situations not yet covered by design conditions).

For the present study, which is on such a double containment reactor building, the PSC IC dome of the present generation 220 MWe capacity Indian NPP (Warudkar, 1997; Chakrabarti and Basu, 1999) has been considered. There the reactor building is composed of two containments (IC and OC) with an annular space separating them from each other. The main components of the IC (Fig. 1) are:

1. PSC cylindrical wall, monolithically built on the raft;
2. PSC spherical dome, with four SG openings at the top of the cylindrical wall and
3. PSC ring beam, at the springing level of the dome (i.e. at the junction of dome and wall).

The IC wall is generally 610 mm thick except for portions near the ring beam, at the junction with the raft and at four prestressing ribs (for

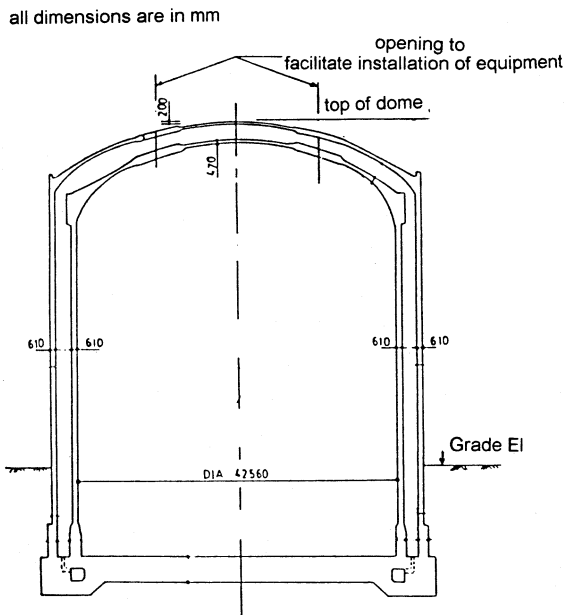


Fig. 1. General arrangement of the two containments.

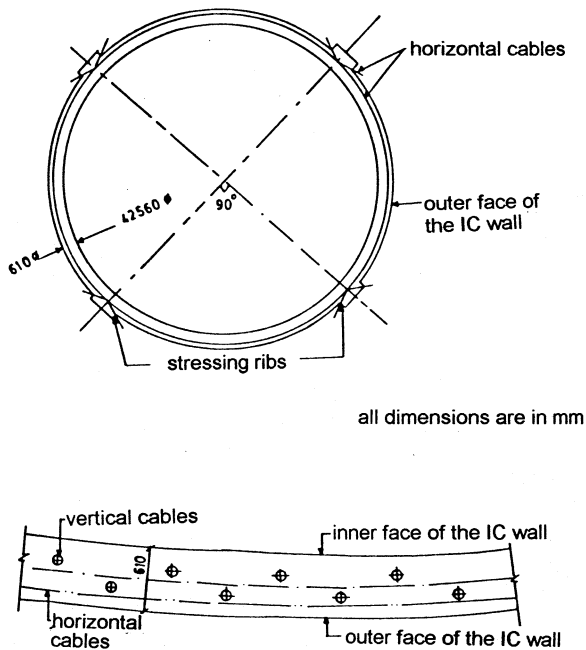


Fig. 2. Horizontal and vertical cable arrangements in the IC wall with stressing ribs.

horizontal prestressing) at right angles extending from top to bottom of the wall. There are vertical prestressing cables from the very bottom of the wall (Fig. 2).

The IC dome has an average thickness of 470 mm, except at springing level and at and around the openings. Two orthogonal layers of prestressing cables composed of the following types are there, with each being a 19K13 HTS strand cable in vertical plane, having a capacity of 355 T UTS.

The prestressing cables are categorized into eight types based on their anchoring/jacking locations. Some of the cables start from the stressing gallery at the junction of the base raft and the cylindrical wall and end up at ring beam at the other side of the dome or at SG opening. Some cables are entirely above the ring beam level; starting from ring beam at one side and ending up at ring beam on the other side or at SG opening. Also there are cables of some other type which extend from one SG opening to another.

The thickness of the dome around the SG openings (each having a diameter 4.1 m) is 1220 mm which is attained through a transition zone of

gradually varying thickness. There are two such thickened portions each encircling two openings with four loop cables (Fig. 3).

The dished head type sealing arrangement is connected to steel embedded plates through welded channels. Embedded and anchored steel plates surround the openings. The top surface plate is anchored with lugs having circular plates at bottom. This annular plate has holes made in it to facilitate placing of concrete and vibration below the plates. The holes are sealed using steel plates after concreting and vibrations. The vertical upper and lower plates are anchored with double legged bars. Between these two plates, there are anchorage pockets made in concrete for anchoring prestressing cables, which, after prestressing, are grouted and sealed with another vertical plate welded to the previous two. The welding is done in such a manner as to ensure no leakage through weld.

### 3. Modeling and analysis

The principle of minimum potential energy has been applied here for the linear elastic F.E. analysis of the structure. Numerically Integrated Elements for System Analysis (NISA), a general purpose F.E. package for a wide spectrum of problems in engineering mechanics, has been used for the present study.

The following types of elements have been used in modeling (NISA User's Manual, 1992). A) 3-D General Shell Element, this element includes membrane, bending and transverse shear deformation effect (i.e. thick shell element), having six degrees of freedom per node (UX, UY, UZ, ROTX, ROTY, ROTZ). The element can be shaped as a four, eight or twelve noded quadrilateral, or a three or six noded triangle depending on the order of the element. The element configuration, node location and face numbering convention for top and bottom surfaces are as shown in Fig. 4. The element may be oriented anywhere in the space, but the connectivity must be given in the order shown in Fig. 4, in which node numbering sequence starts at a corner node and proceeds along the perimeter of the element. For pressure

loading, the pressure is integrated over the area of the loaded face. Stresses can be determined in both local and global systems, at the centroid and/or Gauss points, for the top, middle and bottom surfaces. B) 3-D Beam Element, this is a two node prismatic element including stretching, bending and torsion effects. It has six degrees of freedom per node (UX, UY, UZ, ROTX, ROTY,

ROTZ). The local  $x$ -axis of the element is along the centroidal axis as shown in Fig. 5.

Two different types of mesh, as described below, have been used for modeling the structure, so that the validity of modeling can be checked by comparing the two results obtained using the different meshes. A) Mesh Type 1 (with eight noded 3-D General Shell Element), the whole IC,

all dimensions are in mm

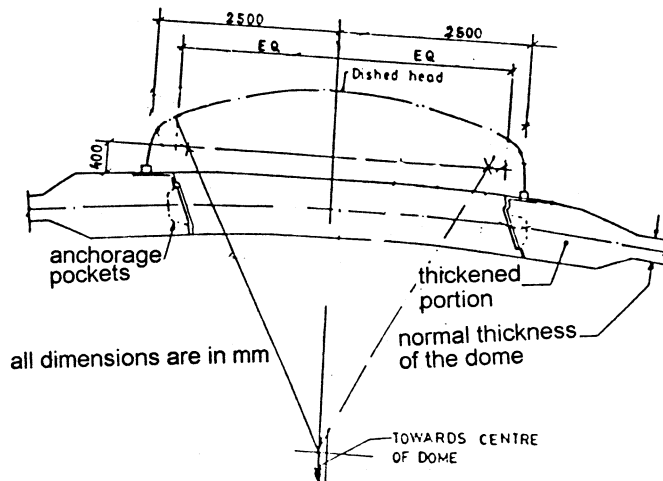
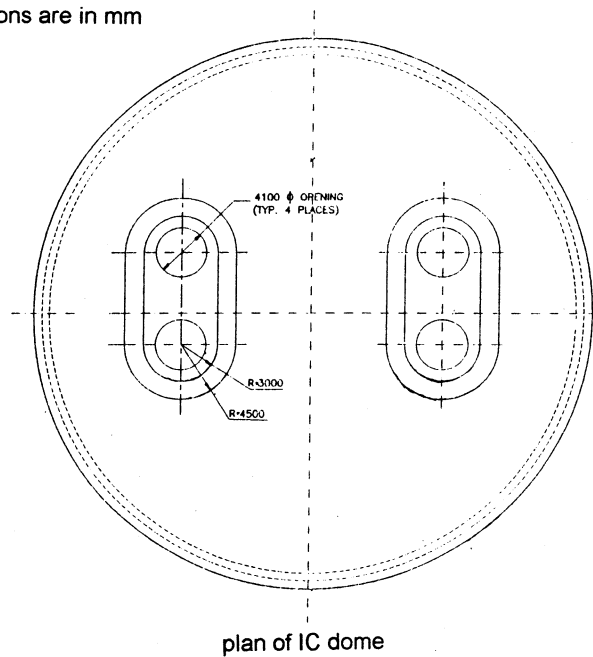


Fig. 3. Section through dome opening.

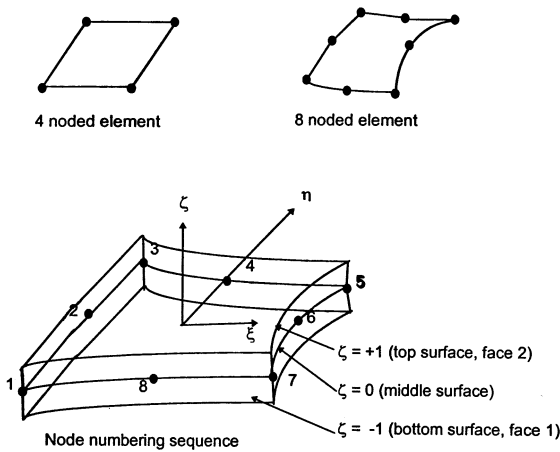


Fig. 4. Element configuration of 3-D general shell element.

from the top of the raft to the full height with SG openings, is discretized with these elements (Fig. 6), where each element node has a thickness same as of the containment at that point. The transition zone of gradually thickening portion (near the SG openings) is simulated by varying the nodal thickness of shell elements. The dished heads (hatch closures) over the SGs have also been modeled with the same elements. The vertical plates are modeled together with 3-D beam elements having their  $x$ -axis along the mid-surface of the shell. The top surface plate is not modeled separately, but its effect is taken by changing the Young's

modulus of the attached shell element to an equivalent one. B) Mesh Type 2 (with four noded 3-D General Shell Element), this mesh differs only in the sense that these four noded elements have been used in stead of those eight noded elements, and these elements, placed parallel to the prestressing cable profile, facilitate in applying the prestressing force directly at the nodes (Fig. 7).

For both the meshes the IC remaining symmetric about one vertical plane, only one of its symmetric halves was analyzed. Fixed boundary conditions ( $UX = UY = UZ = ROTX = ROTY = ROTZ = 0$ ) were applied to all the bottom nodes; and symmetric boundary conditions ( $UX = 0, ROTY = 0$ ) were assigned to all the nodes lying on the plane of symmetry, for both Mesh Type 1 and 2.

The following materials, and their properties, are specified for various parts of the containment structure:

Characteristic strength of concrete for IC wall is M35 (i.e. 28 days cube strength,  $f_{ck} = 35 \text{ N mm}^{-2}$ ), and that for both the IC dome and ring beam is M60. This strength ( $f_{ck}$ ) is related to the other properties of concrete through the following equations (Murali Mohan, 1998):

1. Relation between cylinder strength and cube strength:  $f_{c28} = 0.8f_{ck}$
2. Characteristic tensile strength:  $f_{tj} = 0.6 + 0.06f_{cj}$

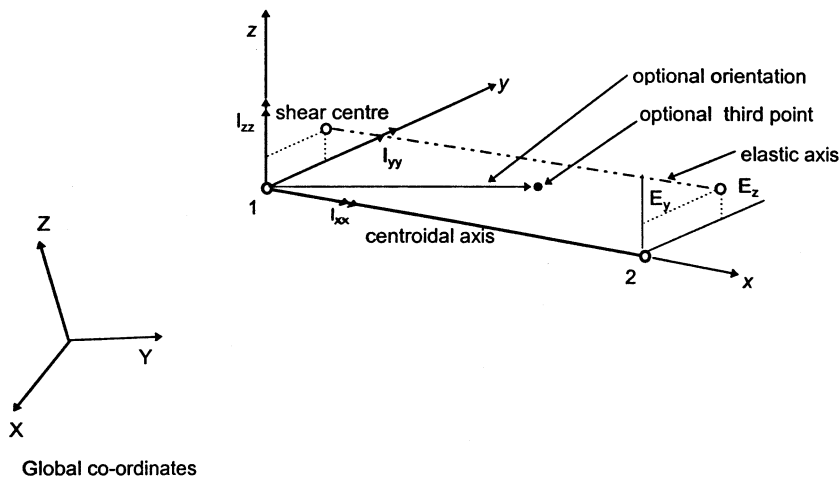


Fig. 5. Element configuration of 3-D beam element.

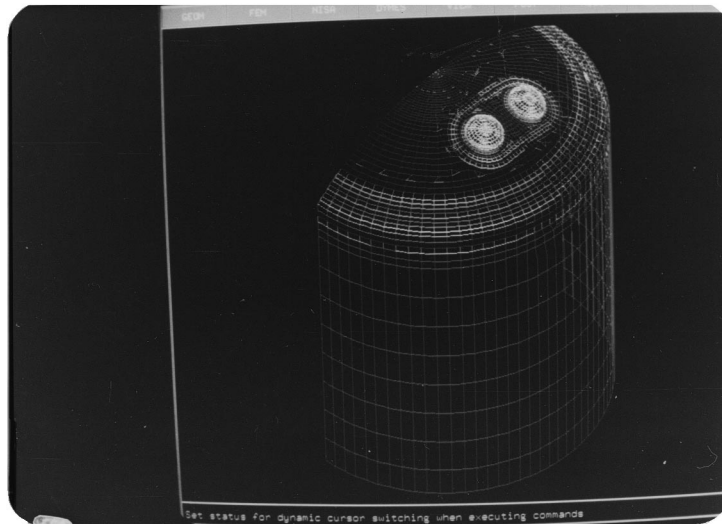


Fig. 6. Isometric view of the finite element Mesh Type 1 of the containment.

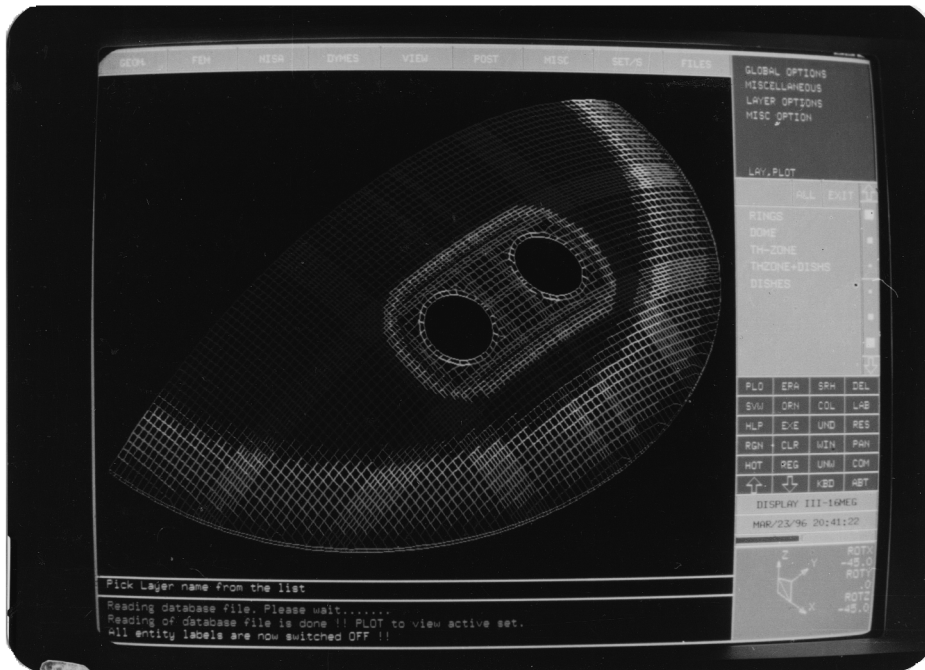


Fig. 7. Detail view of the finite element Mesh Type 2 for dome portion.

3. Modulus of rupture:  $f_{cr} = 0.7\sqrt{f_{ck}}$   
 where,  $f_{cj}$  is the characteristic compressive strength of concrete based on testing of cylinder on  $j$ th day, and,  $f_{ij}$  is the characteristic tensile

strength of concrete based on testing of cylinder on  $j$ th day. Values of  $f_{cj}$  and  $f_{ij}$  for 28 days are 48 and 3.48 MPa, respectively, for M60 grade of concrete, while  $f_{cr}$  is 5.42 MPa. For the present

study the Young's modulus ( $E_c$ ) and Poisson's ratio ( $\nu$ ) are taken (Murali Mohan, 1998) as  $E_c = 5700\sqrt{f_{ck}}$  and  $\nu = 0.2$ , respectively.

The  $E_c$  and  $\nu$  of steel are taken (Murali Mohan, 1998) as 210 GPa and 0.3, respectively.

Also there are various loads which act on the IC, individually or in combination, at different stages of construction and operation. The dead load for concrete is applied by taking its unit weight as  $25 \text{ kN m}^{-3}$ . In addition to that dead load, an average prestressing force of  $2.34 \times 10^6 \text{ N}$  (without deferred loss) is considered to be acting on each cable. This force which is acting along mid-surface of the dome is converted to a uniformly distributed load (u.d.l.) acting radially along the cable profile. This u.d.l. is then converted to nodal point loads along the cable profile, transforming the radial load into three global components at the same time. As the element nodes are along the cable profile for Mesh Type 2 the nodal loads are applied directly. For Mesh Type 1 the nodal loads for cable profile are translated into equivalent nodal loads for the element nodes. At all the anchorage locations an anchorage force of 2.84 MN is applied. An accident pressure of 0.173 MPa (Murali Mohan, 1998) arising out of LOCA/MSLB is applied as outward pressure normal to the inner face of the containment. The test pressure is also same as the accident pressure, both in magnitude and direction.

#### 4. Results and discussions

The results obtained from the analysis are in

the form of static deformation (vertical) and stress (three principal stresses and von Mises stress) contours; for top, middle and bottom layer of the IC dome. These have been obtained for both the mesh types and each for the following two types of loading combination:

1. Dead load + prestress (without hatch closure) and
2. Dead load + prestress + pressure (with hatch closure)

The maximum vertical displacements observed for the two mesh types and for different loading conditions are as shown in Table 1.

The deformation of the IC dome has been observed to be predominately axisymmetric in the regions near the ring beam. The central portion of the dome, including and around SG openings, has been deformed unsymmetrically, possibly due to unsymmetric prestressing forces in the dome along with the relative locations of the SG openings. Fig. 8 and Fig. 9 show this type of output samples clearly.

Figs. 10–13 will show how the different stress contours at some typical layer are obtained from analysis using one mesh type when the structure is acted upon by a given load combination.

Having scrutinized the stress contours for different layers under different loading conditions, it has been apparent that a significant similarity exists in the variation of pattern and magnitude of stresses for a particular stress type under a typical loading condition. For example, the first principal stress contours for Mesh Type 1 under DL + prestress for all the three layers are shown in Figs. 11, 14 and 15. Accordingly, it will be justified to discuss on stress distribution for three layers at a

Table 1  
Maximum vertical displacements in the dome

| Load case                 | Maximum vertical displacement (in mm) |        |                      |
|---------------------------|---------------------------------------|--------|----------------------|
|                           | Mesh-1                                | Mesh-2 | Approximate location |
| Dead load                 | –2.216                                | –2.284 | Near SG opening      |
| Prestress                 | –27.27                                | –27.53 | Near crown portion   |
| Pressure                  | 9.468                                 | 10.05  | Near SG opening      |
| DL + prestress            | –29.22                                | –29.53 | Near crown portion   |
| DL + prestress + pressure | –20.19                                | –19.75 | Near crown portion   |

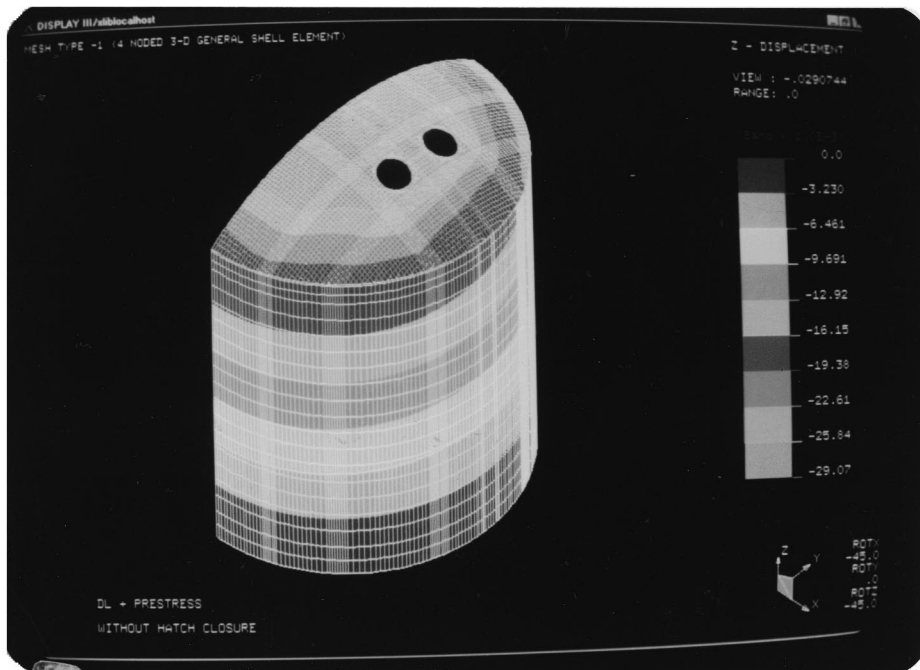


Fig. 8. Vertical displacement contour for DL + prestress for Mesh Type 2.

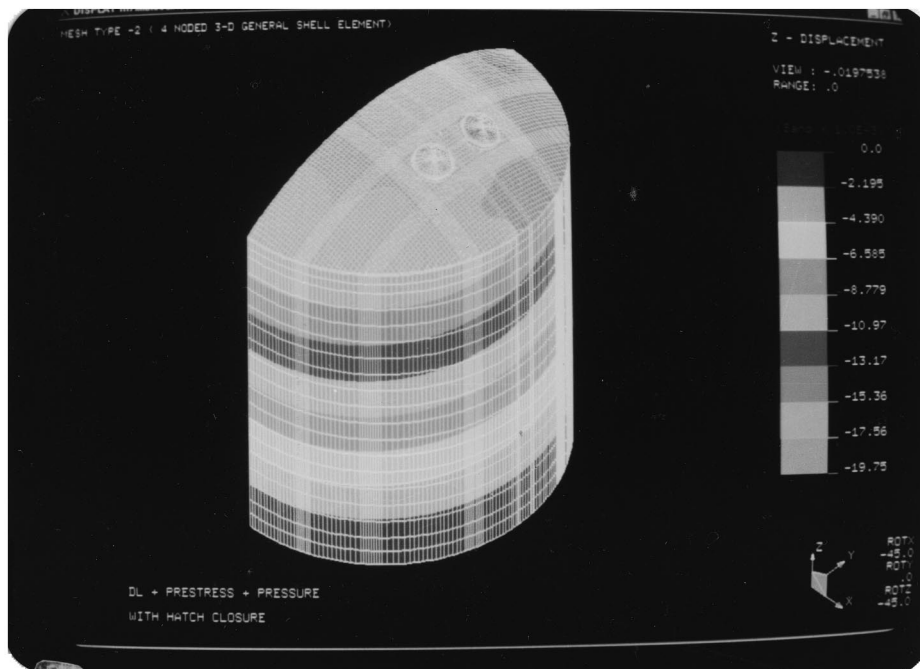


Fig. 9. Vertical displacement contour for DL + prestress + pressure for Mesh Type 2.

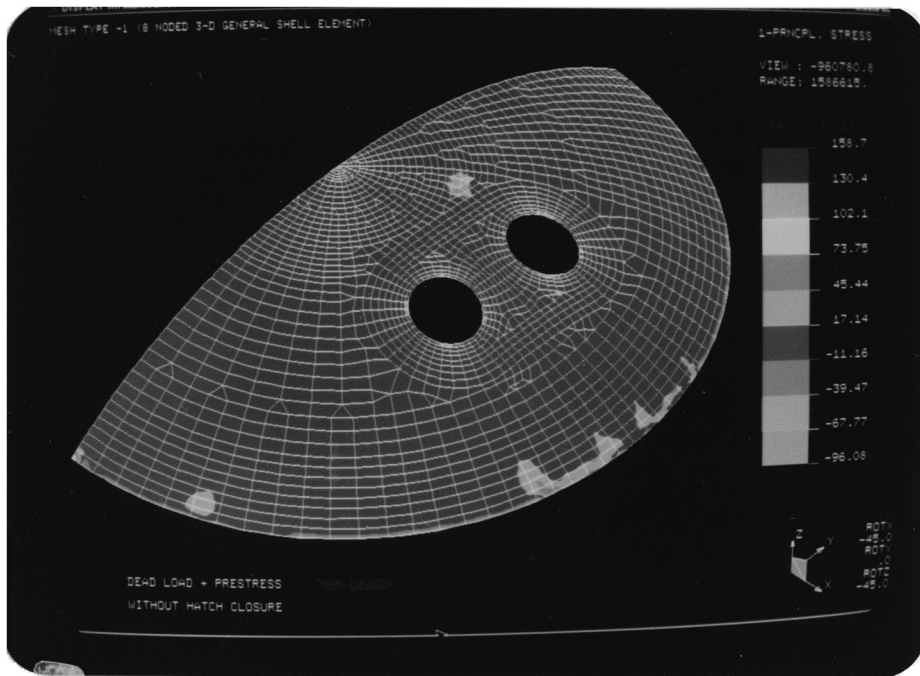


Fig. 10. First principal stress contour at middle layer for DL + prestress for Mesh Type 1.

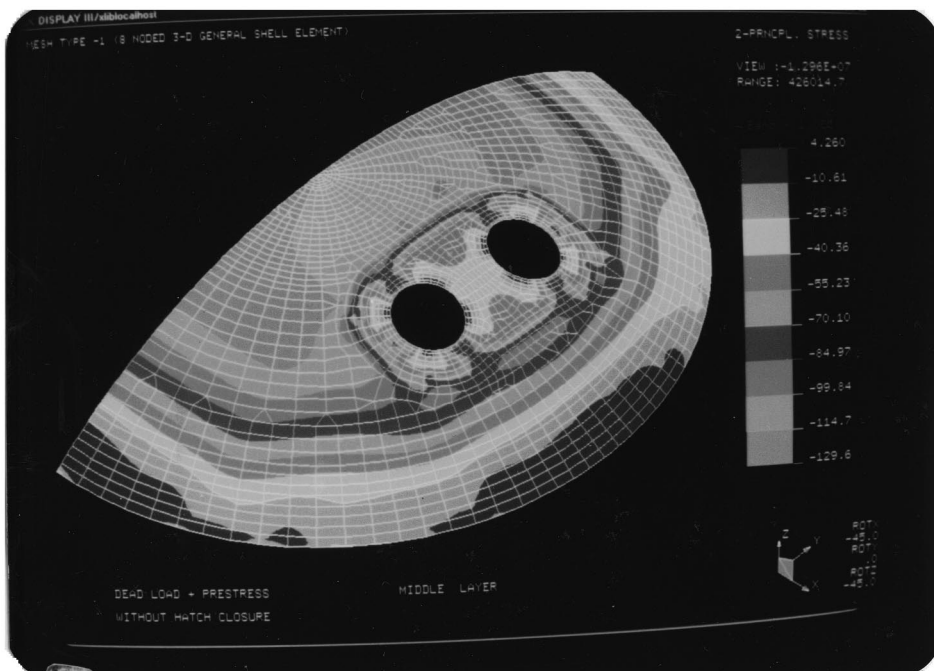


Fig. 11. Second principal stress contour at middle layer for DL + prestress for Mesh Type 1.

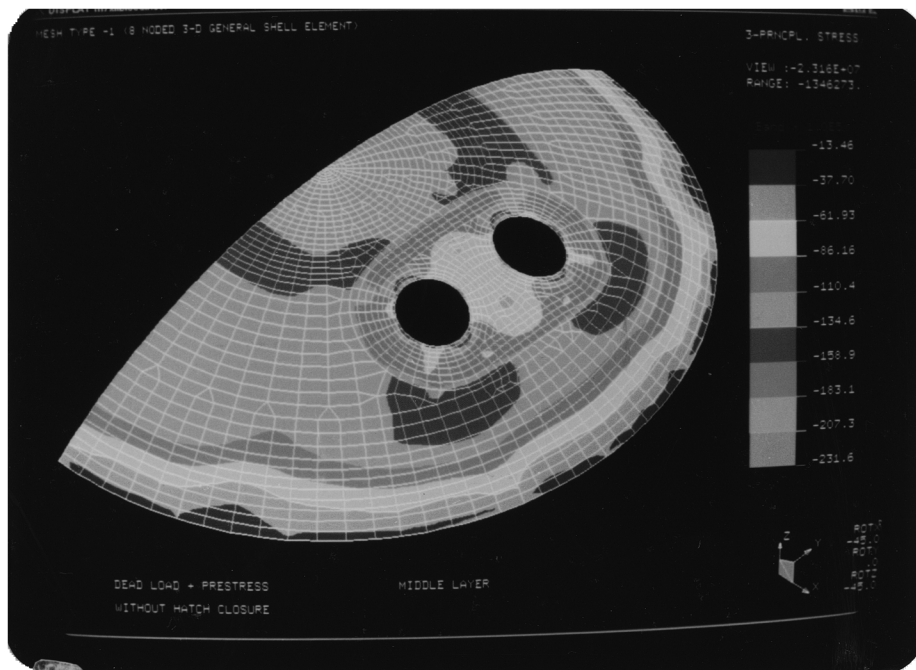


Fig. 12. Third principal stress contour at middle layer for DL + prestress for Mesh Type 1.

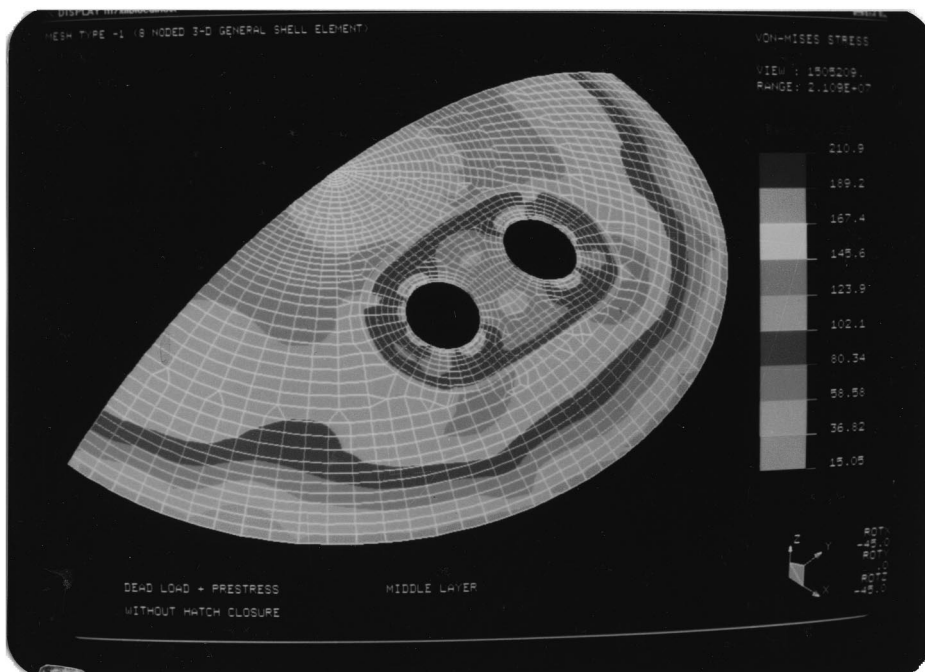


Fig. 13. Von Mises stress contour at middle layer for DL + prestress for Mesh Type 1.

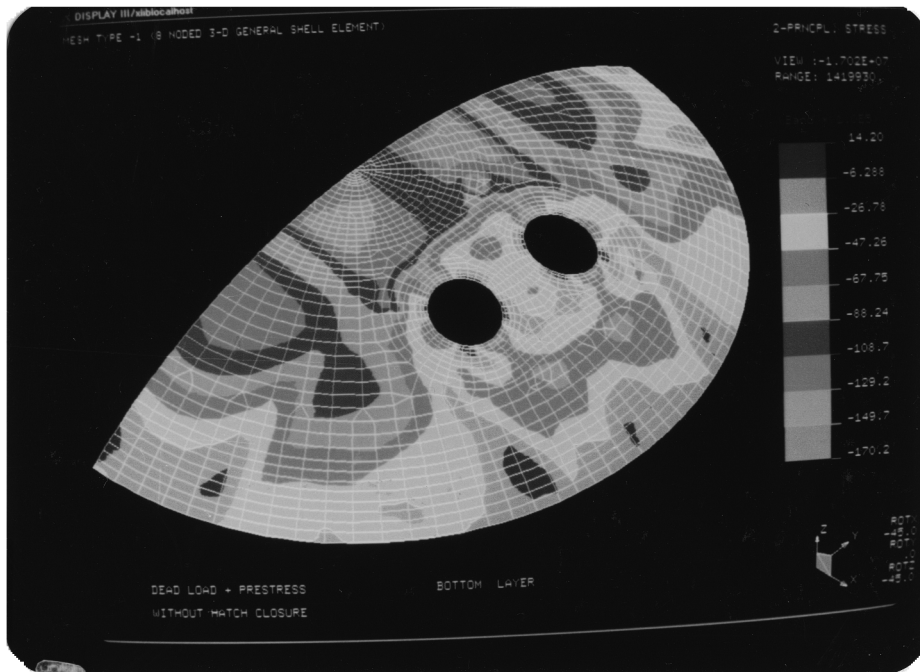


Fig. 14. Second principal stress contour at bottom layer for DL + prestress for Mesh Type 1.

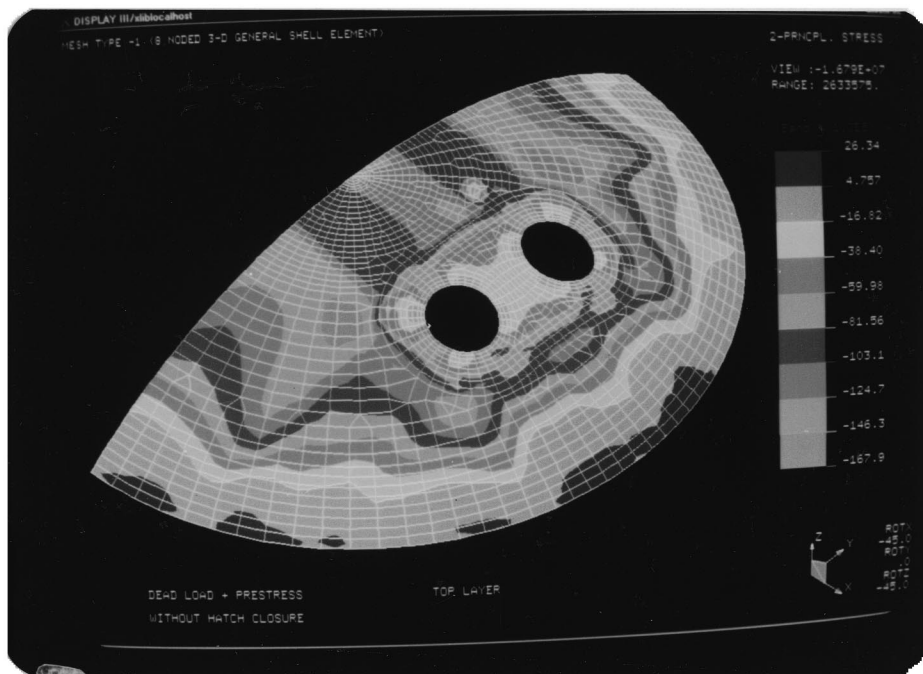


Fig. 15. Second principal stress contour at top layer for DL + prestress for Mesh Type 1.

time for a typical stress due to a typical loading condition.

For the analysis with Mesh Type 1 under DL + prestress the following observations are made.

1. Almost the entire dome has been found to have very low compressive (maximum 0.421 MPa at bottom layer) and tensile (maximum 0.4495 MPa at top layer) first principal stress. But a high value of tensile stress (maximum 5.832 MPa at top layer) occurs at four locations at 45, 135, 225 and 315° at the edges of SG openings (Fig. 18).
2. The second principal stress is compressive at almost all the portion of the dome with uniform thickness of 470 mm (minimum 4.726 MPa at bottom layer and maximum 16.79 MPa at top layer). At the thickened portion the stress decreases and it becomes tensile at some points near ring beam and at the four locations of the SG openings mentioned earlier.
3. The entire dome is under compression for the third principal stress (except for certain regions at the top layer near edge beam having very low values of tension), with the maximum value (maximum 27.61 MPa at bottom layer) at anchorage points at the edges of SG openings.
4. The von Mises stress patterns are also seen to be not much varying at the portions with thickness 470 mm and the magnitude decreases at the thickened portions. But the maximum stress is attained at some points at the thickened edges of the openings (maximum 23.16 MPa at middle layer).

For Mesh Type 1 under DL + prestress + pressure the stress patterns differed from those of the previous loading combination and they are as described below.

1. The dome is predominately under very little first principal compressive (maximum 1.6 MPa at top layer) and tensile (maximum 2.002 MPa at bottom layer) stress. But it is under higher tensile stresses (maximum 8.575 MPa at top layer) at the four locations of each SG opening stated earlier. And a very high tensile stress (maximum 31.28 MPa at bottom layer) at two regions (0 and 180°) at the edge of each SG

opening where the hatch is exactly connected (Fig. 18).

2. The entire portion of the dome with thickness 470 mm is under compressive second principal stress (maximum 8.766 MPa at top layer). The value decreases for the thickened portions and is tensile (maximum 2.034 MPa at middle layer) at some points near the SG openings.
3. The third principal stress in the dome portion having thickness of 470 mm is under compression (maximum 13.15 MPa at top layer). Tension (maximum 0.5122 MPa at top layer) occurs at four locations of the SG openings mentioned previously.
4. The von Mises stress is greater in the thinner portion (maximum 11.76 MPa at top layer) and less at thickened portion (maximum 5.328 MPa at middle layer) of the dome.

Stress contours of these four types each for three layers and under both the loading conditions are obtained again using Mesh Type 2 for analysis. The contours for a typical stress, at a typical layer, for a given load combination, is almost the same for different mesh types, as illustrated in Figs. 16 and 17. So going into the details can be avoided, and for both the meshes it can be summarized with the critical observations written below.

For the loading combination of DL + prestress (without hatch closure) the compressive principal stresses have been in the range of 0–27.61 MPa, with maximum stresses occurring at the prestressing cable anchorage locations around SG openings. Excluding these points the maximum compressive principal stress at the thickened portion surrounding SG boundaries has been found to be around 9.2 MPa. In the remaining portion of the dome (including the ring beam) maximum compressive stress has been found to be about 15 MPa. Principal tensile stress of relatively small magnitudes (maximum up to 2.7 MPa) has been found to occur at some specific locations at the SG boundaries.

For the loading condition of DL + prestress + pressure (with hatch closure) the maximum compressive principal stress is 19.65 MPa, occurring at the anchorage locations around the SG openings. In the rest of the thickened portion the

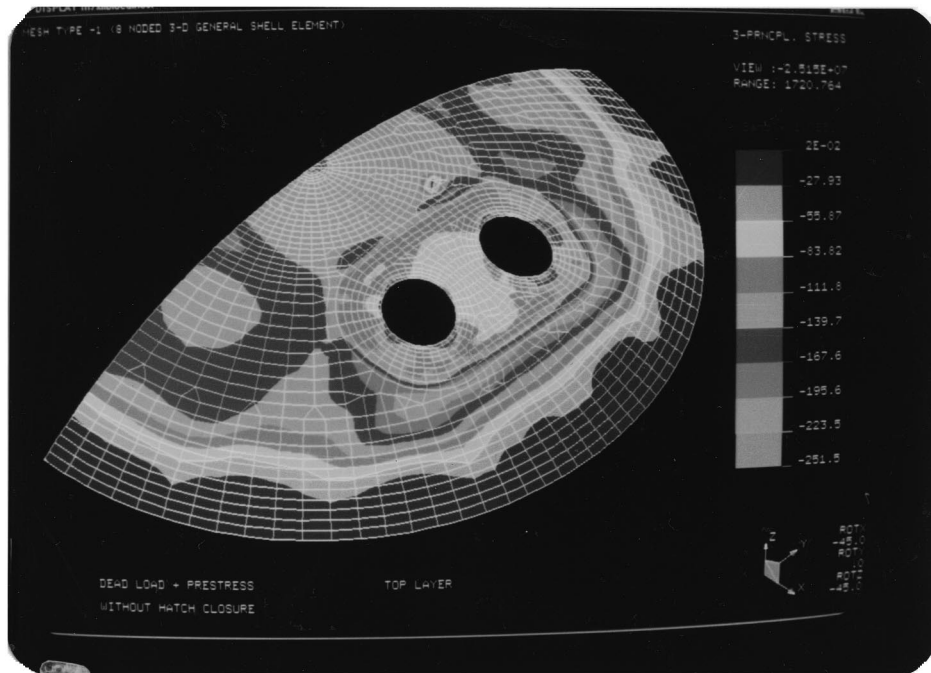


Fig. 16. Third principal stress contour at top layer for DL + prestress for Mesh Type 1.

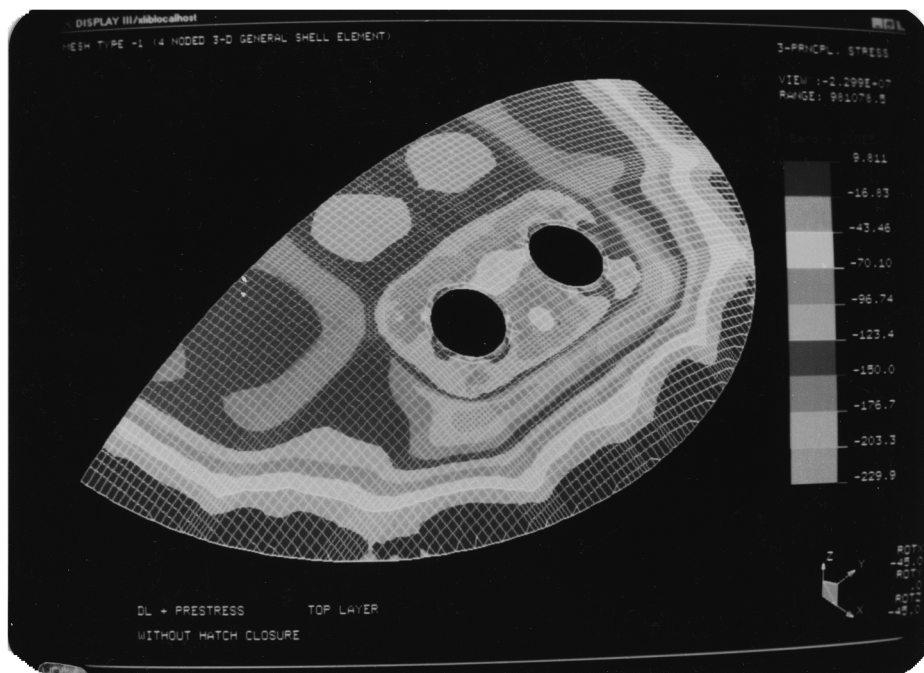


Fig. 17. Third principal stress contour at top layer for DL + prestress for Mesh Type 2.

maximum compression is 6.2 MPa, while it is about 13.1 MPa in the remaining portion of the dome (including the ring beam). Tensile stress of relatively higher magnitudes (maximum up to 8.9 MPa, except for two points at 0 and 180° at the edges of SG openings), compared to the previous loading condition, has been observed here, and at the edges of the SG openings again.

## 5. Conclusions

From detailed study of the results obtained for different loading conditions and different mesh types, the following conclusions have been drawn:

1. The deformation of the IC dome is mainly due to vertical displacement components.
2. The dome undergoes predominately axisymmetric deformations, except for its central region including the thickened portion.

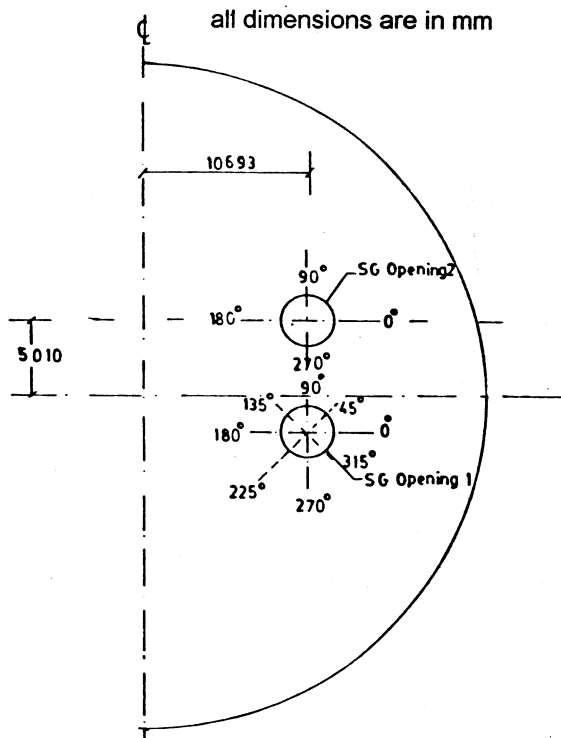


Fig. 18. Plan showing angular locations at the edge of SG openings.

3. Maximum vertical displacement of the dome under DL + prestress is  $\approx 45\%$  higher than that under DL + prestress + pressure.
4. The magnitude of maximum compressive principal stress is within the linear elastic limits of the material, except for some high values in the case of DL + prestress occurring at cable anchorage locations.
5. Significant tensile principal stress has been observed to occur in some specific locations at the edges of SG openings.
6. Variation of stresses at top and bottom layers of the dome signifies that the bending action is dominant at/around SG openings and at the transition zone near the ring beam.
7. Both vertical displacement and stress contours have been found to be almost identical for two types of mesh. There are differences in stress values only at the locations of hatch connection near the edges of SG openings in the case of DL + prestress + pressure (with hatch closure). This comparison is well indicative of the trend of linear behaviour of the PSC IC dome within the framework of assumptions made.

## Acknowledgements

The work reported in this paper is an outcome of the research project, 'Investigation on Performance of Steel-Concrete Interfaces at Penetration Assemblies in the Inner Containment Dome of a Reactor Building', sponsored by the Atomic Energy Regulatory Board, India.

## Appendix A. Nomenclature

|          |   |
|----------|---|
| UX       | displacement along X-axis   |
| UY       | displacement along Y-axis   |
| UZ       | displacement along Z-axis   |
| ROTX     | rotation about X-axis   |
| ROTY     | rotation about Y-axis   |
| ROTZ     | rotation about Z-axis   |
| $f_{ck}$ | characteristic compressive strength of concrete based on testing of cube on 28 days |

|          |  |
|----------|--|
| $f_{cj}$ | characteristic compressive strength of concrete based on testing of cylinder on $j$ th day |
| $f_{tj}$ | characteristic tensile strength of concrete based on testing of cylinder on $j$ th day     |
| $f_{cr}$ | modulus of rupture   |
| $E_c$    | Young's modulus of concrete  |
| $\nu$    | Poisson's ratio of concrete  |
| $\zeta$  | surface number of 3-D shell elements   |

## References

- Chakrabarti, S.K., Basu, P.C., 1999. Issues related to design and construction of prestressed concrete inner containment dome of reactor building with large openings. Proceedings of the 15th International Conference on Structural Mechanics in Reactor Technology, Seoul, Korea.
- Chakrabarti, S.K., Sai A.S.R., Basu, P.C., 1994. Examination of leakage aspects through concrete-steel interfaces at and around containment penetration assemblies. Proceedings of the Third International Conference on Containment Design and Operation, Toronto, Canada.
- Chakrabarti, S.K., Kumar, A., Basu, P.C., 1997. Leakage through concrete-steel interfaces at and around containment penetration assemblies: some new observations. Proceedings of the Second International Conference on Advanced Reactor Safety, Orlando, FL, USA.
- Harrop, L.P., 1984. Stress distribution around the equipment hatch opening for a prestressed concrete containment for a PWR power station, structural engineering in nuclear facilities (vol. 2). Proceedings of the conference sponsored by the Committee on Nuclear Structures and Materials of the Structural Division of the ASCE, pp. 828–846.
- Murali Mohan, K., 1998. Linear behaviour of PSC inner containment dome with penetrations of a reactor building. M. Tech. Thesis, Indian Institute of Technology, Kanpur, India.
1992. NISA User's Manual, (vol. 1 and 2). EMRC, Bangalore, India.
- Task Group on Containment Capability, 1984. ASCE Materials and Structural Design Committee, Structural Engineering in Nuclear Facilities (vol. 2). Proceedings of the conference sponsored by the Committee on Nuclear Structures and Materials of the Structural Division of the ASCE, pp. 948–1012.
- Warudkar, A.S., 1997. Nuclear power plant containment design: evolution and Indian experience. Joint WNO/OECD-NEA Workshop, Prestress Loss in NPP Containments, Civaux NPP, Poitiers, France.